Cell

Orchestrated Intron Retention Regulates Normal Granulocyte Differentiation

Justin J.-L. Wong,[1,4,8] William Ritchie,[1,2,4,8] Olivia A. Ebner,[5] Matthias Selbach,[5] Jason W.H. Wong,[6] Yizhou Huang,[6] Dadi Gao,[1,2,4] Natalia Pinello,[1,4] Maria Gonzalez,[1,4] Kinsha Baidya,[1,4] Annora Thoeng,[1,4] Teh-Liane Khoo,[1,4] Charles G. Bailey,[1,4] Jeff Holst,[1,3,4,9] and John E.J. Rasko[1,4,7,9,*]

[1]Gene and Stem Cell Therapy Program
[2]Bioinformatics Laboratory
[3]Origins of Cancer Laboratory
Centenary Institute, Camperdown 2050, Australia
[4]Sydney Medical School, University of Sydney, NSW 2006, Australia
[5]Max-Delbrück Centre for Molecular Medicine, Berlin 13125, Germany
[6]Lowy Cancer Research Centre and the Prince of Wales Clinical School, University of New South Wales, Sydney 2052, Australia
[7]Cell and Molecular Therapies, Royal Prince Alfred Hospital, Camperdown 2050, Australia
[8]These authors contributed equally to this work
[9]These authors contributed equally to this work
*Correspondence: j.rasko@centenary.org.au
http://dx.doi.org/10.1016/j.cell.2013.06.052

SUMMARY

Intron retention (IR) is widely recognized as a consequence of mis-splicing that leads to failed excision of intronic sequences from pre-messenger RNAs. Our bioinformatic analyses of transcriptomic and proteomic data of normal white blood cell differentiation reveal IR as a physiological mechanism of gene expression control. IR regulates the expression of 86 functionally related genes, including those that determine the nuclear shape that is unique to granulocytes. Retention of introns in specific genes is associated with downregulation of splicing factors and higher GC content. IR, conserved between human and mouse, led to reduced mRNA and protein levels by triggering the nonsense-mediated decay (NMD) pathway. In contrast to the prevalent view that NMD is limited to mRNAs encoding aberrant proteins, our data establish that IR coupled with NMD is a conserved mechanism in normal granulopoiesis. Physiological IR may provide an energetically favorable level of dynamic gene expression control prior to sustained gene translation.

INTRODUCTION

Alternative splicing of RNA affects almost all multiexonic genes to promote genetic diversity (Black, 2000; Pan et al., 2008). Of the three modes of RNA splicing that also include exon skipping and alternative splice site usage; intron retention (IR) is the least understood. IR is a form of alternative splicing that occurs when an intron, having been transcribed as part of a pre-mRNA, is not spliced out, thus resulting in an otherwise mature mRNA retaining an unprocessed sequence. Intron-retaining transcripts often contain a premature termination codon (PTC) and are therefore either targeted for degradation by the nonsense-mediated decay (NMD) pathway or their expression is restricted to the nucleus (Lejeune and Maquat, 2005). As a result, IR has been overlooked as a means of normal gene regulation (Bicknell et al., 2012; Hillman et al., 2004) despite isolated instances of IR-associated biological function (Bell et al., 2008, 2010; Buckley et al., 2011).

Careful dissection of the molecular circuitry controlling myelopoiesis has served as a paradigm for cellular differentiation. Lineage commitment toward granulopoiesis begins with the hemopoietic stem cell losing its ability to self-renew, and the stepwise acquisition of specific myeloid identity (Rosenbauer and Tenen, 2007). The terminal phases of myeloid development are marked by distinct transcriptional and translational changes, including changes in the expression of cell surface markers (Novershtern et al., 2011; Theilgaard-Mönch et al., 2005; Ward et al., 2000). These are accompanied by unique changes in the shape and size of the cell, including dramatic changes leading to a multilobular nucleus in the final stage of granulopoiesis (Lee et al., 1999). Although this unique morphological change has been extensively studied, its mechanisms remain unknown.

Although removal of PTC containing transcripts by NMD is essential for the normal development of hemopoetic stem and progenitor cells (Weischenfeldt et al., 2008), the extent of IR coupled with NMD has not been explored. To investigate the impact of alternative splicing, and specifically IR in granulopoiesis, we performed massively parallel mRNA sequencing (mRNA-seq) and mass spectrometry on pure populations of promyelocytes, myelocytes, and mature granulocytes isolated from murine bone marrow. Because loss of mRNA following NMD and the abundance of low complexity regions in introns make it difficult to quantify IR, we developed an algorithm, IRFinder, which detects changes in levels of IR between two samples from mRNA-seq data. Bioinformatic analysis of our data revealed a unique pattern of alternative IR accumulation in genes involved in granulocyte function and nuclear morphology (including *Lmnb1*), leading to decreased protein levels in granulocytes. Inhibition of NMD using caffeine treatment or

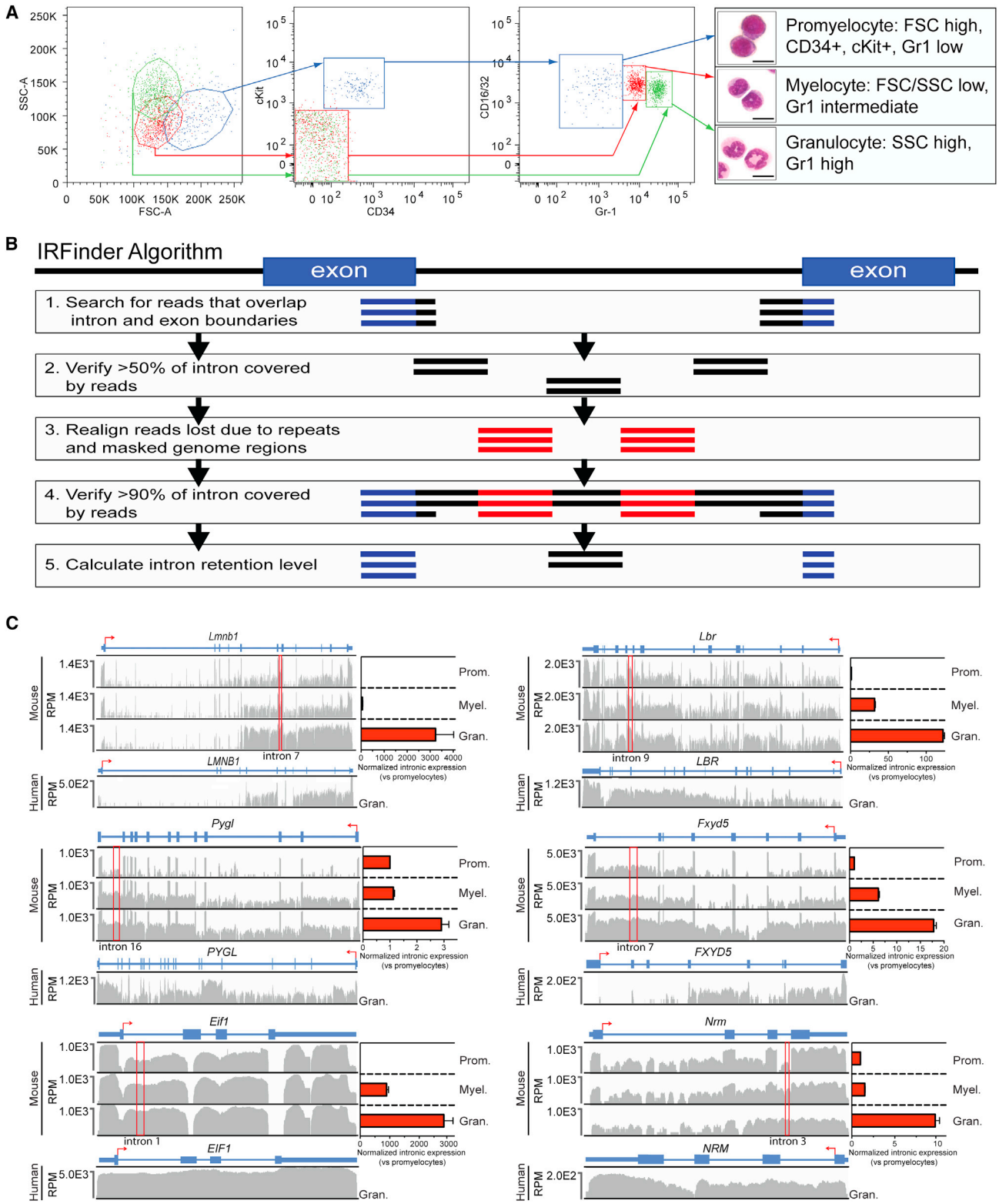

Figure 1. Intron Retention Is a Widespread Phenomenon Conserved between Human and Mouse

(A) Representative flow cytometry plots and May-Grünwald Giemsa staining showing FACS enrichment strategy of murine promyelocytes, myelocytes, and granulocytes from bone marrow. Scale bar, 10 μm.

(B) Schematic of the five step approach utilized by the IRFinder algorithm to calculate intron retention levels. See also Figure S5.

(legend continued on next page)

knockdown of the core NMD factor, *Upf1*, resulted in the accumulation of intron-retaining transcripts, indicating that IR triggered NMD. Re-expression of *Lmnb1*, which expressed one of the highest levels of IR in mouse bone marrow, significantly altered granulocyte nuclear shape, size, and peripheral granulocyte numbers, suggesting that programmed IR is a critical regulatory pathway in normal granulocyte development.

RESULTS

Specific Patterns of Intron Retention Are Observed during Granulopoiesis

To study IR in sequential stages of granulopoiesis, we performed mRNA sequencing (mRNA-seq) and mass spectrometry on primary mouse promyelocytes, myelocytes, and granulocytes purified using fluorescence activated cell sorting (FACS) (Figures 1A and S1A available online). Bioinformatic analysis (see Experimental Procedures) of the mRNA-seq data from polyA-enriched RNA showed 2,432 differentially regulated genes (Table S1), of which 563 were transcribed into 948 alternatively spliced isoforms with significant changes in expression between promyelocytes and granulocytes ($p < 0.05$, Audic and Claverie Test (Audic and Claverie, 1997) (Table S2). We created an algorithm called IRFinder (Figure 1B) to discover retained introns and highlight differentially retained introns between paired samples. We found 121 introns transcribed from 86 genes (Table S3) that were retained at significantly different levels between promyelocytes and granulocytes ($p < 0.05$, Audic and Claverie Test (Audic and Claverie, 1997). Of these 86 genes, 30 displayed alternative IR in multiple introns. In order to validate our mRNA-seq data, we used quantitative reverse transcription PCR (RT-qPCR) with primers specific to both introns and correctly spliced exons for 20 of these intron-retaining transcripts detected by IRFinder. By measuring the ratio of intronic expression normalized to exonic expression, we directly confirmed IR in 80% (16/20) of these transcripts (Figures 1C and S1B). mRNA-seq performed on human granulocytes identified IR in the same genes shown in Figure 1C (see Intron Retention Is Conserved between Human and Mouse) for human data). These intron-retaining transcripts were polyadenylated and highly enriched in the cytoplasm (Figure 2), confirming that they are fully processed and exported mRNAs rather than splicing intermediates. 83/86 (97%) intron-retaining mRNAs contained at least one PTC (Table S3), making them putative candidates for degradation via the NMD pathway (Belgrader et al., 1994; Hentze and Kulozik, 1999).

Heatmaps of expression levels for the 121 retained introns and 948 alternatively spliced isoforms in mouse promyelocytes, myelocytes, and granulocytes revealed striking differences between alternative splicing and IR (Figure 3A). Non-IR alternative splice isoforms displayed dynamic changes in expression, with some isoforms being highly expressed in only the middle stage of differentiation, predominantly in the first and last stages or in gradients. In contrast, IR predominantly accumulated during differentiation, with low levels in promyelocytes, increasing through myelocytes to the highest levels in granulocytes. Distinct patterns of isoform versus intron-retaining transcript expression suggested that they are differentially regulated. We also noticed that groups of introns from the same transcript were either concomitantly spliced out or retained (Figures 1C and S1B). This sets IR apart from other types of splicing in which different exons of the same transcript may be included or excluded independently.

We next determined whether alternatively expressed genes were enriched for specific Gene Ontology categories (Figures 3B and S2). As expected, functions specific to granulocytes were significantly represented (Figure 3B). Notably, IR, but not total gene expression or alternative splicing, was significantly associated with the nuclear periphery and nuclear lamina (Figure 3B). This suggests that IR may regulate remodeling of the nuclear envelope and shape, which are unique characteristics of granulocytic differentiation.

To determine the proportion of intron-retaining transcripts versus correctly spliced transcripts, we calculated the median number of reads that mapped to retained introns against those that mapped to all known transcripts for each IR gene correcting for length and total mappable reads in each sample (Figure 3C). We found that over 25% of all transcripts from 24 genes retained introns.

Intron Retention in Granulopoiesis Is Associated with a Drop in Expression of Splicing Factors Responsible for Exon-Intron Definition and High Intronic GC Content

To determine whether changes in the splicing machinery may be a mechanism responsible for IR, we analyzed the mRNA expression and protein levels of small nuclear ribonuclear protein genes belonging to each of the major spliceosomal complexes (Kanehisa et al., 2012). The majority of the U1 and U2 subunits were downregulated (up to 125-fold) during granulopoiesis (Figure 3D), whereas the other subunits were mostly stable (Figure 3E). Protein levels of Sf3b1, for example, which has been recently shown to be essential for intron definition (Shao et al., 2012), decreased 7-fold. This indicated that IR may arise from the downregulation of spliceosomal components that are responsible for the recognition of intron and exon boundaries, especially at the branch point and the 5′ extremity of the intron, but not the subsequent stages of lariat formation and cleavage.

A recent report identified differential GC content between introns and exons as essential for spliceosomal recognition (Amit et al., 2012). Introns with high relative GC content use a mode of splicing that involves intron definition rather than exon definition. In this "intron definition" mode of splicing, changes in splicing efficiency are more likely to result in a retained intron rather than skipped exons. We calculated intronic and flanking

(C) mRNA-seq reads (normalized per total number of mappable reads, RPM) in promyelocytes (prom.), myelocytes (myel.), and granulocytes (gran.) are portrayed on the same scale using IGV v2.1 software for murine genes *Lmnb1*, *Lbr*, *Pygl*, *Fxyd5*, *Eif1*, and *Nrm*. mRNA-seq data of orthologous human genes (uppercase) in granulocytes is displayed beneath. Sequence reads (vertical gray lines), translational direction (red arrow: note use of alternate strands in *Fxyd5*/*FXYD5* and *Nrm*/*NRM* with conservation of IR toward the 3′-end), exons (dark blue boxes), and introns (blue horizontal lines) are shown. RT-qPCR was used to compare the expression of retained introns (red boxes) to flanking exons during granulocyte differentiation. Data are from three independent experiments each in triplicate and show mean ± SEM normalized to the expression in promyelocytes. See also Figure S1.

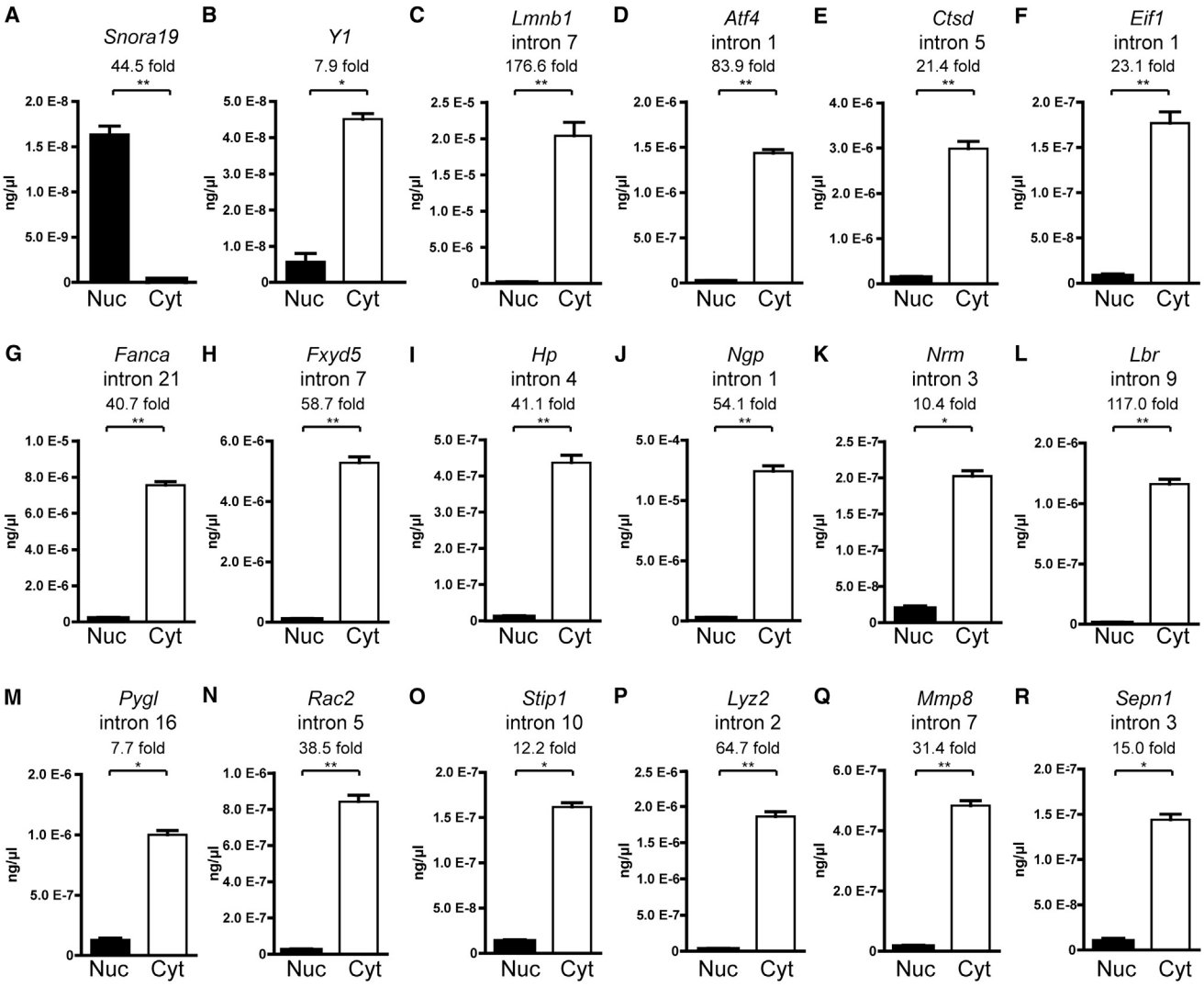

Figure 2. Expression of Intron-Retaining Transcripts in the Nuclear and Cytoplasmic Fractions of Granulocytes Demonstrates that They Are Processed and Exported

(A–R) Enrichment of control genes, *Snora19* (A) and *Y1* (B) in the nucleus (Nuc) and cytoplasm (Cyt), respectively, indicates the purity of the nuclear and cytoplasmic fractions. Expression of intron-retaining mRNA transcripts of *Lmnb1* (C), *Atf4* (D), *Ctsd* (E), *Eif1* (F), *Fanca* (G), *Fxyd5* (H), *Hp* (I), *Ngp* (J), *Nrm* (K), *Lbr* (L), *Pygl* (M), *Rac2* (N), *Stip1* (O), *Lyz2* (P), *Mmp8* (Q), and *Sepn1* (R) was measured in the cell-equivalent amount of nuclear and cytoplasmic RNA. Fold differences between the expression of transcripts in the nuclear and cytoplasmic fractions are shown above. Data are from three independent experiments each in triplicate and show mean ± SEM. Two-tailed Mann Whitney U-test was used to determine significance, denoted by * ($p < 0.05$), ** ($p < 0.001$).

exonic GC content for IR genes and for all other genes expressed during granulopoiesis (Figure 3F). We found significantly higher GC content in retained introns compared to spliced introns in both mouse and human mRNA-seq data (Figure 3F, see Intron Retention Is Conserved between Human and Mouse for human data). This finding leads us to believe that IR genes operate through a model of intronic recognition, making them more susceptible to IR than other genes.

Intron Retention Coupled with Nonsense-Mediated Decay Suppresses Protein Levels during Granulopoiesis

To determine the consequences of IR, we first investigated whether intron-retaining transcripts can escape NMD and undergo translation. Incorrect recognition of translation termination, which allows translational stop codon readthrough or translation reinitiation has been shown to bypass NMD (Neu-Yilik et al., 2011; Zhang and Maquat, 1997). We investigated the presence of these mechanisms of NMD escape by attempting to map our mass spectrometry data from the same cell extracts to intronic sequences and to the 3′UTR of intron-retaining genes. We found that 6,031 mass spectra mapped to the coding region of genes with IR but no spectra mapped to introns or 3′UTRs of these genes, suggesting that proteins are not produced when IR occurs (Table S4). Thus, intron-retaining transcripts do not escape NMD, either via translation reinitiation or stop codon readthrough.

To assess whether small noncoding RNAs, such as microRNAs, were being expressed from retained introns, we performed small RNA-seq on primary mouse promyelocyte, myelocyte, and granulocyte samples. We found no known microRNA or hairpin-like small RNA expressed from within retained introns (Table S5), ruling out the possibility that their expression determines granulocytic differentiation.

To directly test whether IR triggers NMD, the NMD pathway was inhibited using caffeine in combination with actinomycin D (Ivanov et al., 2007) and accumulation of intron-retaining transcripts was measured by whole-genome expression analysis. Treatment of cells with caffeine leads to downregulation of SMG1, a member of the phosphatidylinositol 3-kinase-related protein kinase family (Yamashita et al., 2001) known to inhibit the phosphorylation of the core NMD factor, UPF1, thereby blocking the NMD pathway. Of the 86 genes that exhibited differential IR, 75 had higher levels of IR in granulocytes; 39 of 86 showed significantly increased expression levels after caffeine treatment ($p < 0.05$, RUV procedure described in Experimental Procedures with Holm-Bonferroni correction). Although caffeine treatment is known to have pleiotropic effects including upregulation of alternatively spliced isoforms (Shi et al., 2008) in addition to NMD blockade (Ivanov et al., 2007), the identification of the 39 intron-retaining genes represented a significant enrichment ($p < 0.05$, Fisher's exact test). Because IR leading to NMD would result in decreased mRNA, and therefore decreased protein levels, we examined our mass spectrometry data to determine protein expression. Mass spectrometry data were available for 21 out of these 39 IR genes, with 18/21 showing reduced protein levels when IR was highest ($p = 0.0015$, binomial test), further suggesting that IR leads to NMD and consequently reduced gene expression during granulopoiesis (Table S6).

Intron Retention Is Conserved between Human and Mouse

To assess whether IR is also an important regulatory mechanism conserved in human granulopoiesis, we performed mRNA-seq on human granulocytes and measured the extent of IR. Using IRFinder, we found 855 genes expressed in human granulocytes in which at least one intron was retained (Table S7). Of the 86 genes that exhibited differential IR during murine granulopoiesis, 71 were expressed in human granulocytes, and 36 of these showed IR. This significant overlap ($p = 2.85 \times 10^{-22}$, hypergeometric test) between human and mouse genes demonstrated that IR was conserved. To investigate whether conservation of IR was due to sequence homology between human and mouse genes, we measured the levels of intron retention of "orthologous introns" among the 36 genes with conserved IR. Despite our demonstration that this is a conserved process within genes, there was no correlation in the levels of IR for orthologous introns in each gene.

Intron Retention of *Lmnb1* Leads to Nonsense-Mediated Decay-Regulated Loss-of-Protein Expression during Mouse Granulopoiesis

To confirm the biological function of IR during granulopoiesis, we selected Lmnb1, a key nuclear protein, for further analysis. *Lmnb1* was among three genes (*Lmnb1*, *Lmnb2*, and *Lbr*) linked to nuclear structure in granulocytes and showed one of the highest levels of differential IR using mRNA-seq (Figures 1C and 3C), as well as downregulation of protein levels measured by mass spectrometry (Table S6). Our mRNA-seq data revealed high levels of IR across multiple introns of the *Lmnb1* gene in mature murine granulocytes, whereas much less intron retention was detected in promyelocytes or myelocytes (Figure 1C). Using RT-qPCR (Figure 4A), over 100-fold greater retention of introns five to ten was detected in mature granulocytes compared to promyelocytes. Introns one to four were not differentially retained in any of the three stages of granulopoiesis (Figure 4A), confirming the specificity of this mechanism.

Higher levels of IR correlated with the downregulation of correctly spliced mRNA transcripts by up to 100-fold (Figure 4A) and low levels of protein expression (Figures 4B and 4C) of Lmnb1 in myelocytes and granulocytes. Immunofluorescence demonstrated the loss of Lmnb1 expression at the nuclear membrane (Figure 4C). Consistent with data from primary cells, we demonstrated accumulation of *Lmnb1* introns during all-*trans* retinoic acid-induced differentiation of the MPRO cell line into granulocytes, and this change also correlated with a decrease in spliced mRNA expression (Figure 4D). These results suggest that the function of IR is to reduce *Lmnb1* expression in maturing granulocytes.

To determine whether *Lmnb1* transcripts with retained introns were degraded by NMD, this pathway was inhibited using caffeine coupled with actinomycin D (Ivanov et al., 2007), and accumulation of intron-retaining transcripts was measured by RT-qPCR (Figure 5A). A significant accumulation of *Lmnb1* mRNA with retained introns was found in primary promyelocytes, myelocytes, and granulocytes treated with caffeine, with the highest level observed in granulocytes (Figure 5B). Accumulation of intron-retaining *Lmnb1* transcripts was also observed in differentiated MPRO cells (Figure 5C). For both primary myeloid and MPRO cells, there was a significant increase in the level of retained introns 7 and 8 after caffeine treatment during differentiation, compared to the level of native IR (Figures 4A and 4D) in each sample (Prom:Myel $p < 0.0003$; Myel:Gran, $p < 0.0475$; Control:ATRA, $p < 0.0001$). Due to the possible pleiotropic effects of caffeine, we also performed siRNA knockdown of *Upf1* in primary granulocytes (Figure 5D), which resulted in a significant accumulation of intron-retaining *Lmnb1* mRNA and other intron-retaining transcripts shown in Figure 1C (Figure 5E), thus confirming the results of caffeine treatment. Importantly, expression of correctly spliced mRNA transcripts was not elevated following inhibition of NMD using either approach (Figures 5B, 5C, and 5E). These data suggest that IR-coupled NMD is a specific mechanism involved in the degradation of mRNA transcripts including *Lmnb1* that failed to splice out introns in maturing granulocytes.

Downregulation of *Lmnb1* and Other Intron-Retaining Transcripts Is Not Attributable to Transcriptional Regulation

To examine the contribution of transcriptional regulation in the control of IR gene expression, we determined the levels of nascent transcripts for 36 intron-retaining genes and known

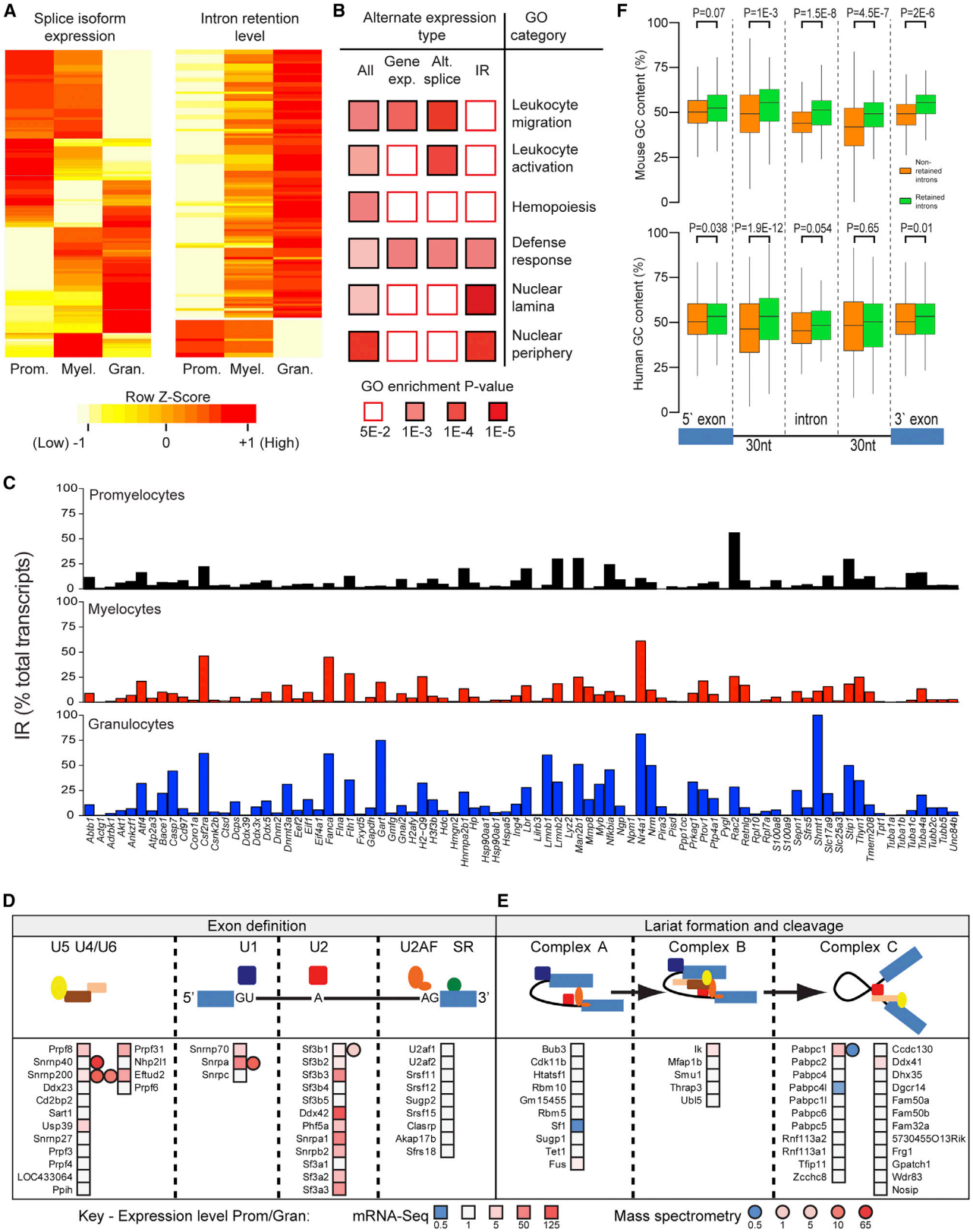

(legend on next page)

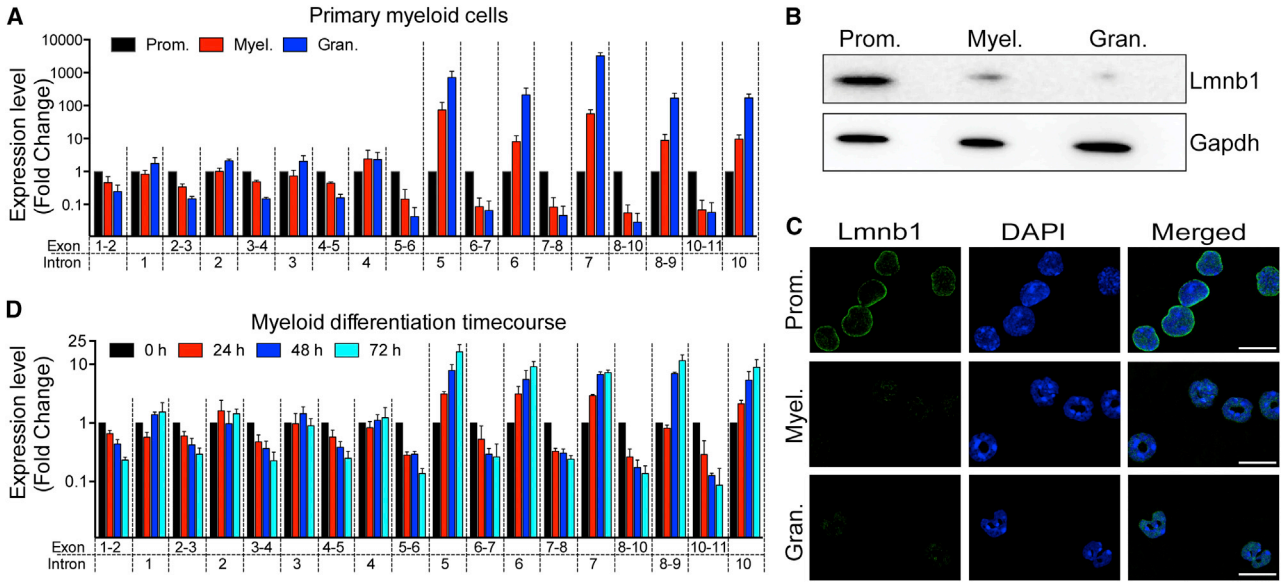

Figure 4. Intron Retention of *Lmnb1* Is Associated with the Loss of mRNA and Protein Expression during Granulopoiesis In Vivo and In Vitro

(A) RT-qPCR showing the expression levels of introns 1–10 and flanking exon junctions of *Lmnb1* during granulocyte differentiation.

(B) Western blot analysis showing reduced Lmnb1 protein expression during granulopoiesis. Gapdh was the loading control.

(C) Expression and localization of Lmnb1 protein using immunofluorescence (green). Progressive loss of Lmnb1 was observed during primary granulopoiesis. Nuclei were detected using DAPI (blue). Scale bar, 10 μm.

(D) MPRO cells were differentiated with ATRA and intron-retaining *Lmnb1* transcripts were assessed for introns and flanking exon junctions using RT-qPCR. Data are from three independent experiments each in triplicate and show mean ± SEM.

transcriptionally regulated controls during granulopoiesis (Guibal et al., 2009). For known transcriptionally downregulated genes including *Ctsg*, *Ela2*, *Flt3*, *Mpo*, *Myc*, and *Prtn3*, nascent transcript expression decreased by up to 100-fold from promyelocytes to granulocytes (Figure 6A). Nascent transcript expression of genes known to be transcriptionally upregulated, such as *Ltf*, *Cebpd*, and *Mmp9*, increased by up to 1,000-fold (Figure 6A). Notably, nascent transcript expression of 36 intron-retaining genes including *Lmnb1* was either stable, slightly downregulated (by 1–2 fold) or increased from promyelocytes to granulocytes (Figure 6B). These data indicate that the reduced expression of intron-retaining genes is not due to altered transcription. Downregulation of *Lmnb1* and other intron-retaining genes is more likely attributable to IR coupled with NMD with little or no impact exerted by transcriptional regulation.

Lmnb1 Expression during Granulopoiesis In Vivo Affects Hemopoiesis, Granulocyte Nuclear Shape, and Nuclear Volume

To elucidate whether Lmnb1 loss was required for granulocyte development and nuclear structure, we expressed *Lmnb1* that could not retain introns in an immune competent mouse bone marrow transplant model using retroviral-mediated gene transfer. Lmnb1 expression levels in granulocytes engineered to express intronless Lmnb1 were comparable to that of normal mouse promyelocytes (Figure S3). Control (empty vector) and Lmnb1 expression vectors resulted in similar engraftment rates as determined by the percentage of GFP coexpression in the bone marrow, blood, and spleen (Figure 7A). Lmnb1-expressing granulocyte cell concentrations were significantly decreased in the peripheral blood at 4 and 10 weeks posttransplantation compared to controls (Figures 7B and 7C).

Figure 3. Intron Retention Measured in Granulocyte Differentiation Displays a Unique Pattern of Expression and Controls Functionally Related Genes

(A) Heatmaps displaying the expression level of transcripts with non-intron-retaining alternate splice isoforms (left) and transcripts with alternate intron retention (right) during the three stages of granulopoiesis. See also Tables S1, S2, and S3.

(B) Gene Ontology (GO) analysis of the significantly overrepresented categories (p values with Benjamini-Hochberg correction) linked to leukocyte functions for all observed changes in transcript expression and for each subcategory of alternate expression. See also Figure S2 for the number of genes and overlap within GO categories for each type of alternative transcription.

(C) Percentage of transcripts from IR genes with at least one retained intron from mRNA-seq data.

(D and E) The mechanism contributing to retention of introns includes reduced expression of RNA and protein of essential splicing factors. Numerous factors specific to exon definition are downregulated (D), whereas factors specific to lariat formation and cleavage (E) are mostly stable. The upper panels represent specific components and stages of splicing.

(F) GC content was measured for introns and flanking exons of mouse and human genes that retained introns (Table S7) versus correctly spliced genes.

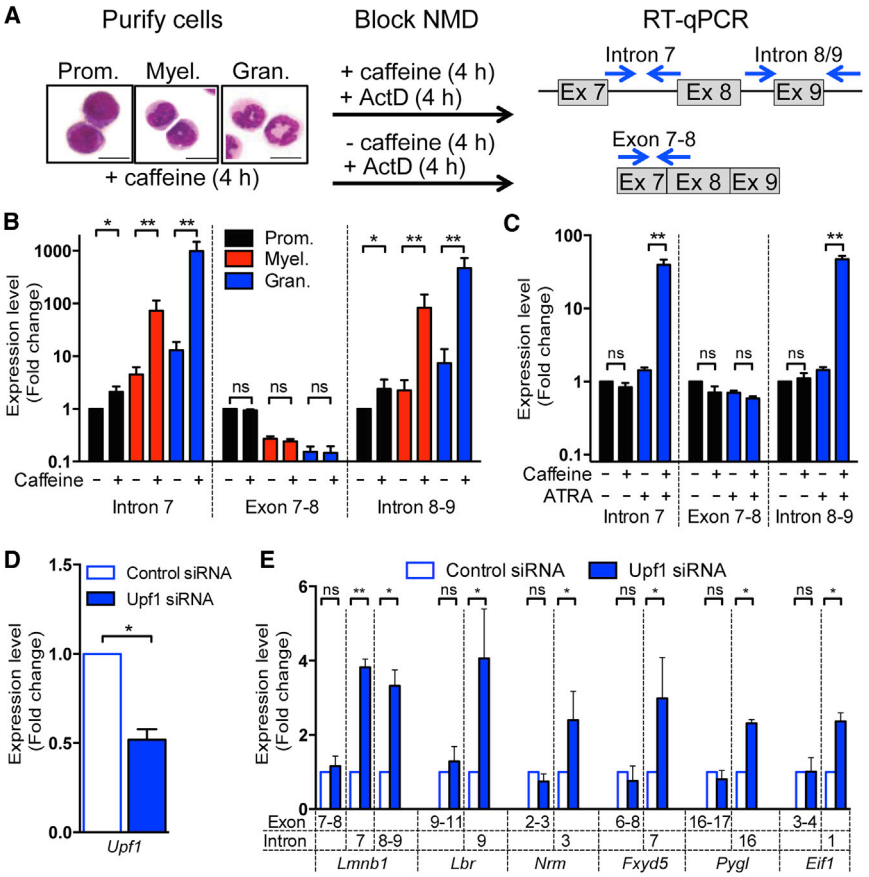

Figure 5. Inhibition of Nonsense-Mediated Decay in Primary Myeloid and MPRO Cells Demonstrates that Intron Retention Is a Physiological Event that Reduces Gene Expression

(A) Schematic showing protocol used to block nonsense-mediated decay (NMD) in mouse primary myeloid cells using caffeine and actinomycin D (ActD) followed by RT-qPCR of *Lmnb1*.

(B) Results of caffeine protocol to block NMD in primary mouse cells, followed by *Lmnb1* RT-qPCR to determine IR levels.

(C) Caffeine-induced accumulation of intron-retaining and spliced *Lmnb1* transcripts was assessed in MPRO cells differentiated by ATRA for 72 hr.

(D) Levels of *Upf1* mRNA detected in unenriched primary granulocytes at 24 hr posttransfection with Upf1 siRNA compared to control.

(E) Levels of intron-retaining and adjacent spliced exons of *Lmnb1*, *Lbr*, *Nrm*, *Fxyd5*, *Pygl*, and *Eif1* mRNA in granulocytes following *Upf1* knockdown compared to siRNA control measured by qRT-PCR. Two-tailed Mann Whitney U-test was used to determine significance, denoted by * ($p < 0.05$), ** ($p < 0.001$) and ns (not significant). Data are from three independent experiments each in triplicate and show mean ± SEM. Prom., promyelocytes; Myel., myelocytes; Gran., granulocytes.

Analysis of purified GFP$^+$ granulocytes (>95% purity) by immunofluorescence showed Lmnb1 protein expression was exclusively localized in the membrane of characteristically lobulated granulocyte nuclei, in contrast to control granulocytes that lacked expression (Figures 7D and S3B). Furthermore, the shape and size of the nucleus was altered in Lmnb1-expressing granulocytes assessed by May-Grünwald Giemsa or DRAQ5 staining (Figure 7E). To quantify the increase in nuclear volume, purified GFP$^+$ granulocytes were stained with DRAQ5 and analyzed using deconvolution microscopy combined with image analysis. The nuclear volume of Lmnb1-expressing granulocytes was significantly increased (~30%) compared to controls (n = 212 cells per group; $p < 0.0001$; Figures 7E and 7F, and Movie S1). Despite the altered nuclear morphology, there were no effects on purified GFP$^+$ granulocyte cell function assessed by nitro blue tetrazolium assay (Figure S4A). Analysis of the nuclear lamina structure by transmission electron microscopy showed no differences between purified control and Lmnb1-expressing granulocytes (Figures S4B–S4E).

DISCUSSION

In the present study, we used computational analysis of mRNA-seq data coupled with mass spectrometry to monitor gene expression and protein levels during differentiation of highly purified myeloid cells. We developed an algorithm, IRFinder, to discover alternately retained introns in mRNA-seq data. This algorithm incorporates two features: a round of mapping to an unmasked genome and use of the median of read counts that map to introns. Mapping to an unmasked genome ensures that certain introns containing low complexity regions were not excluded from IR analysis. A median count of mapped reads ensures that peaks of expression from within introns do not artificially inflate estimated levels of IR (Figure S5). We demonstrate that IR regulates numerous genes, including *Lmnb1*, which are involved in the unique changes observed in nuclear structure during the terminal phase of granulocytic differentiation. The level of IR of these genes increases markedly during each stage of differentiation, resulting in greatly reduced protein levels. This mechanism of gene expression control appears to be transcriptionally independent because we did not observe downregulation of nascent transcripts of IR genes during granulocyte differentiation (Figure 6). The consistent pattern of increasing retention of introns distinguishes it from other types of alternative splicing which display more disparate patterns (Figure 3A). Orthologous gene pairs that displayed conserved IR rarely retained the same introns suggesting that IR is a conserved mechanism of gene regulation that may have evolved for specific genes. We also noted a 3′ bias in intron retention, presumably due to degradation that begins at the 5′ end.

Our data indicated that increased numbers of retained introns during granulopoiesis were associated with downregulation of splicing factors responsible for exon recognition. Our sequencing and mass spectrometry analyses detected marked

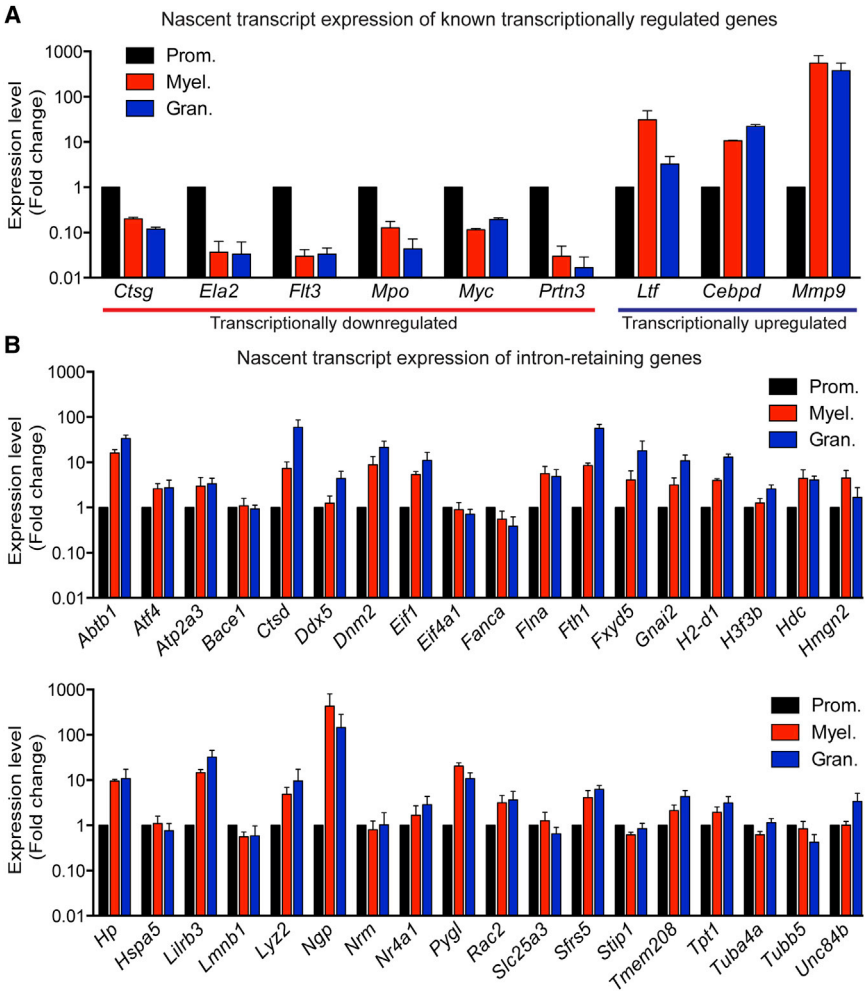

Figure 6. Analysis of Nascent RNA Transcripts Confirms the Lack of Transcriptional Regulation in Reducing the Level of Expression of Intron-Retaining Genes

(A and B) Histograms show expression levels of nascent transcripts of known transcriptionally downregulated or upregulated genes (A) and IR genes (B) in promyelocytes, myelocytes, and granulocytes. Data are from three independent experiments each in triplicate and show mean ± SEM. Prom., promyelocytes; Myel., myelocytes; Gran., granulocytes.

downregulation of the Snrpa subunit of U1snRNP (over 50-fold, Figure 3D) during granulocyte differentiation. Snrpa binds the stem loop II of U1snRNA, and this interaction is essential for subsequent binding to other snRNPs, including U2 to regulate splicing (Shao et al., 2012). Depletion of U1snRNP is known to inhibit pre-mRNA splicing (Kaida et al., 2010; Padgett et al., 1983), and the stoichiometry of U1snRNP has recently been shown to be important in determining mRNA length, isoform expression, and IR (Berg et al., 2012). It is plausible that altered levels of the U1snRNP complex or other snRNPs are responsible for less efficient splicing, which leads to IR. Our model is also supported by the high levels of GC content in retained introns compared to introns that are spliced out of expressed genes (Figure 3F). This indicates that an ''intron recognition'' mode is perhaps being utilized. Thus, decreased splicing factors may selectively lead to intron retention in a subset of genes with high intronic GC content. Further experiments are required to directly prove that retention of GC-rich introns are responsible for driving destabilization of the transcripts through NMD. In particular, it would be interesting to determine whether re-insertion of individual introns into the cDNA constructs (from Figure 7) leads to IR. This could determine whether the GC content of an individual intronic sequence is sufficient to cause IR; however, it remains possible that either a specific intron and/or multiple introns are required, or that exonic sequences can also contribute to IR signals within an individual gene.

Our results extend recent work demonstrating that IR affects some genes, but not others (Berg et al., 2012; Kaida et al., 2010). Factor(s) controlling the specificity for retention of particular introns remain to be clarified but may include epigenetic factors such as histone modifications (Alló et al., 2009; Luco et al., 2010), noncoding RNAs (Beltran et al., 2008; Kishore and Stamm, 2006), and the presence of retrotransposon-containing sequences (Buckley et al., 2011; Lev-Maor et al., 2008), which are known to regulate splicing. Notably, intron-retaining transcripts in dendritic cells are enriched with ID elements, a class of SINE retrotransposon (Buckley et al., 2011).

Our present data reveal downregulation of Lmnb1 and other nuclear envelope proteins during mouse granulopoiesis, consistent with previous findings in human granulocytes (Olins et al., 2001, 2008). We showed that this is mediated by IR, which results in the degradation of intron-retained *Lmnb1* mRNA by the NMD pathway, rather than by transcriptional regulation (Figures 5 and 6). LMNB1/Lmnb1 forms a framework with multiple nuclear proteins such as LMNB2/Lmnb2 and NPM1/Npm1 to provide structure and stability to the nucleus (Dechat et al., 2008; Houben et al., 2007; Ji et al., 2007) and facilitate chromatin remodelling, DNA replication, repair, and transcription (Malhas et al., 2007, 2010; Peric-Hupkes et al., 2010; Tang et al., 2008). Although mouse embryonic fibroblasts lacking wild-type *Lmnb1* do not exhibit altered nuclear shape or stiffness (Ji et al., 2007; Lammerding et al., 2006), studies performed in diverse differentiated cells have demonstrated distorted or blebbed nuclei (Lammerding et al., 2006; Martin et al., 2009; Vergnes et al., 2004; Yang et al., 2011). Human *LMNB1* downregulation has also been shown to inhibit cell proliferation (Shimi et al., 2011), thus it is plausible that IR-induced downregulation

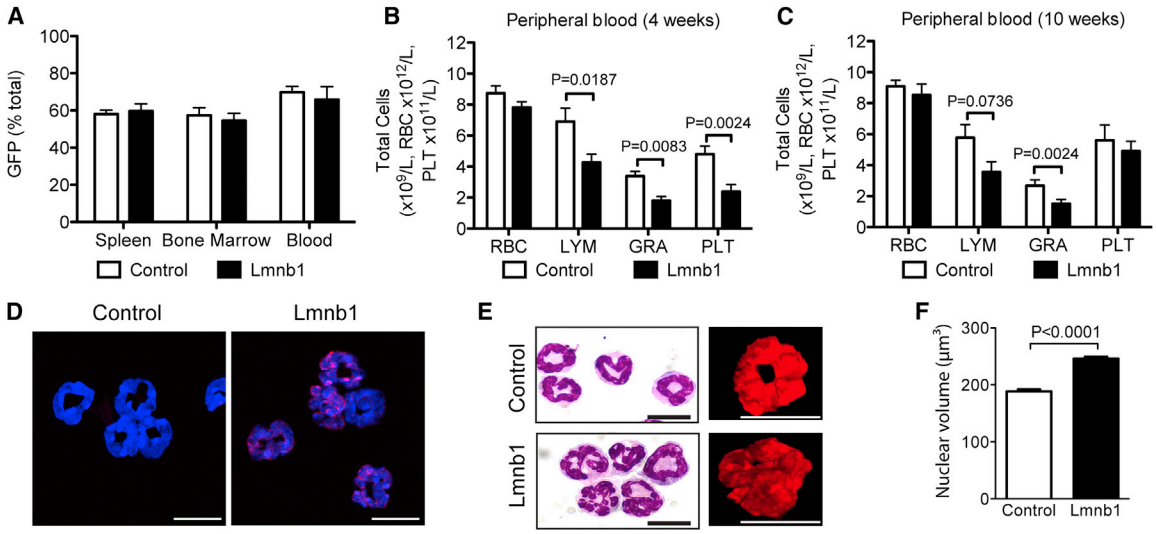

Figure 7. Hemopoietic Reconstitution Experiment Reveals that Preventing Intron Retention in *Lmnb1* Affects Granulocyte Numbers, Nuclear Size, and Shape

(A–E) Intronless Lmnb1 and GFP, or control and GFP, were coexpressed in mouse bone marrow cells using retrovirus-mediated gene transfer. (A) Bone marrow and spleen were isolated and analyzed for GFP expression by flow cytometry to demonstrate equal reconstitution. GFP expression (A) and cell numbers were analyzed in peripheral blood subsets after 4 (B) or 10 (C) weeks. Red blood cells (RBC), lymphocytes (LYM), granulocytes (GRA), and platelets (PLT) were examined, with significance determined using a two-tailed Mann Whitney U-test. GFP-expressing granulocytes were purified by FACS, fixed, and examined by immunofluorescence for Lmnb1 expression (D), May-Grünwald Giemsa and DRAQ5 staining for nuclear morphology (E). Projections of a rendered nucleus of representative control and Lmnb1-expressing granulocytes stained with DRAQ5 are shown at right in red (see Movie S1 for 3D view).

(F) Nuclear volume of granulocytes following DRAQ5 staining was determined using Volocity 3D image analysis software (n = 212), with significance determined using a two-tailed Student's t test.

All graphs show mean values ± SEM. Scale bars in (D) and (E) represent 10 μm. See also Figures S3 and S4.

of *Lmnb1* may be associated with reduced proliferation and consequent differentiation into mature granulocytes.

We have demonstrated the effect of enforcing intronless *Lmnb1* expression in mouse granulocytes to a level that is comparable to normal promyelocytes (Figure S3). We showed that there was a significant decrease in granulocytes in the peripheral blood of mice overexpressing *Lmnb1*, demonstrating that normal granulopoiesis was perturbed (Figures 7B and 7C). Our data revealed an alteration in the nuclear structure and volume of granulocyte nuclei following persistence of *Lmnb1* expression during the terminal phases of granulocytic differentiation (Figures 7D–7F). Although re-expression of Lmnb1 led to significant changes in nuclear morphology, it is likely that downregulation of a network of nuclear membrane proteins, including but not limited to lamin proteins, may be required to facilitate the normal lobulation and formation of characteristic doughnut-shaped nuclei in mature murine granulocytes (Houben et al., 2007; Peric-Hupkes et al., 2010). This unique morphological characteristic of granulocytes is thought to facilitate migration of granulocytes through tight tissue spaces in the event of infection (Hoffmann et al., 2002). Morphological changes reminiscent of those shown in Figure 7E are observed in megaloblastic anemia. We provide evidence that IR of *Lmnb1* leads to smaller nuclei, which may be important to ensure efficient granulocyte differentiation or distribution.

Several specific examples strongly suggest that IR is a physiological phenomenon diversely required for particular biological functions in neurons and dendritic cells (Bell et al., 2010, 2008; Buckley et al., 2011), the regulation of the Vitamin D signaling and in *Arabidopsis* (Kalyna et al., 2012). Our current study has dramatically expanded the repertoire of orchestrated IR coupled with NMD under normal physiological conditions, highlighting its role in the regulation of 86 genes involved in the immune response, and specifically including nuclear lamina genes.

Overall, we provide a comprehensive bioinformatic analysis and experimental validation of global changes in gene expression during granulopoiesis, which has uncovered a transcriptionally independent regulatory role for IR and consequent NMD in controlling protein expression levels. The possible adaptive advantage of IR-coupled NMD as another mechanism of gene expression regulation has not previously been determined. IR may downregulate gene expression faster than transcriptional regulation as observed with other posttranscriptional and translational mechanisms (Hobert, 2008). Because transcription is predicted to consume much less energy than translation, this possible adaptive layer of regulation can be achieved without major metabolic costs (Schwanhäusser et al., 2011). Orchestrated IR and NMD could also play a role in the differentiation of other tissue types.

EXPERIMENTAL PROCEDURES

Primary Cell Isolation and Cell Culture

Bone marrow was harvested from the femur, tibia, and spine of C57BL/6J mice using a mortar and pestle in phosphate-buffered saline (PBS) supplemented with 2% (v/v) fetal calf serum as previously described (Holst et al., 2006a).

Purified populations of promyelocytes, myelocytes, and granulocytes were isolated from murine bone marrow using FACS on a BD Aria II (Figure 1A). $CD11b^{+}CD15^{+}$ human granulocytes were isolated using FACS. MPRO were cultured and differentiated as previously described (Lian et al., 2002).

RNA Isolation and mRNA- and Small RNA-Seq

Total RNA was extracted from cells using Trizol and the RNA quality was confirmed using RNA 6000 Nano Chips on an Agilent 2100 Bioanalyzer (Agilent Technologies). mRNA- and small RNA-seq were performed by Geneworks (Adelaide) using an Illumina GAIIx platform. Poly-A-enriched mRNA libraries were prepared from 20 μg of total RNA using TruSeq RNA sample prep kit (Illumina), according to the manufacturers' instructions. Small RNA libraries were prepared from 5 μg of RNA using the Small RNA Sample Preparation Alternative v1.5 Protocol (Illumina), according to the manufacturers' instructions.

Bioinformatic Analyses and Intron Retention Discovery

mRNA-seq reads were mapped to the mouse genome NCBI m37 using Bowtie 0.12.7 (Trapnell et al., 2010). Alternative transcription start sites and gene expression were determined using Cufflinks Version 0.92. Alternative splicing was measured using a method described in Sultan et al., (2008) and using mouse exon coordinates from the Ensembl Genome Browser Version 58. An algorithm called IRFinder was designed to detect intron retention (IR) and measure variations in the level of specific IR between samples (Figure 1B). Please refer to Extended Experimental Procedures for details.

In comparing human and mouse data we wished to determine the extent of IR in orthologous introns. Because of the high number of repeat elements and low complexity sequences present in introns, we identified orthologous introns by searching for flanking orthologous exons. Exons were considered orthologous if they were the reciprocal best match using blast (Altschul et al., 1990) from the blastall (v 2.2.2.21) package with default parameters among all exons in the respective genome. We defined the introns between these orthologous exon pairs as orthologous introns.

Small RNA structures were folded using RNAfold (Hofacker, 2009) from the Vienna package with default parameters (Table S5). Gene ontology enrichment was performed using the DAVID website (Huang et al., 2009). GO categories with a p value < 0.05 after Benjamini Hochberg correction were considered significant.

Caffeine Treatment and Gene Expression Analysis

Treatment of cells with caffeine was performed as previously described (Ivanov et al., 2007). Messenger RNA expression in caffeine-treated and control cells was determined using Affymetrix GeneChip Gene 1.0 ST mouse arrays according to the manufacturers' instructions. For RT-qPCR, total RNA samples were treated with DNase I, amplification grade (Invitrogen). cDNA was generated using SuperScript III First-Strand Synthesis System (Invitrogen), according to the manufacturers' instructions. RT-qPCR was performed using the CFX96 Real Time PCR Machine (Bio-Rad). Reactions were performed in 20 μl volumes containing 1 × IQ SyberGreen supermix and 0.3 μM of the respective forward and reverse primers. Cycling conditions were: 95°C for 6 min followed by 95°C for 30 s, primer-specific annealing temperature for 30 s, and extension at 72°C for 30 s. Primer sequences for all RT-qPCR reactions are shown in Table S8.

Knockdown of Upf1 in Primary Granulocytes

FACS-purified granulocytes from C57BL/6J mice were transfected with 150 nM Upf1 or negative control siRNA using the human $CD34^{+}$ Cell Nucleofector Kit (Lonza) according to the manufacturers' instructions. Sequences of Upf1 and negative control siRNA were previously published (Ni et al., 2007).

Isolation of Nuclear and Cytoplasmic RNA

Nuclear and cytoplasmic RNAs were isolated from sorted granulocytes using the PARIS kit (Ambion) with RNase inhibitors to minimize RNA degradation as previously described (Taft et al., 2010).

Analysis of Nascent RNA Transcripts

Nascent RNA transcripts were captured using the Click-iT Nascent RNA Capture Kit (Invitrogen). In brief, FACS-purified mouse promyelocytes, myelocytes and granulocytes were labeled with 0.2 mM 5-ethynyl uridine (EU) for 16 hr. EU-labeled nascent RNA was extracted, biotinylated and captured according to the manufacturers' instructions. Captured nascent RNA was converted to cDNA using the SuperScript VILO cDNA Synthesis Kit (Invitrogen) according to the manufacturers' instructions followed by RT-qPCR. Primer sequences are shown in Table S8.

Bone Marrow Transduction and Transplantation

The mouse *Lmnb1* cDNA was cloned into the pMIG vector, and GP+E86 packaging cells were generated for retroviral transduction of mouse bone marrow cells as previously described (Holst et al., 2006a, 2006b).

Microscopy, Immunofluorescence, Immunoblotting, and Mass Spectrometry

Microscopy, immunofluorescence, immunoblotting and mass spectrometry (Tables S4 and S6) were performed using standard protocols and are detailed in the Extended Experimental Procedures.

ACCESSION NUMBER

The National Center for Biotechnology Information Gene Expression Omnibus number for mRNA sequencing and array data sets described in this study is GSE48307.

SUPPLEMENTAL INFORMATION

Supplemental Information includes Extended Experimental Procedures, five figures, eight tables, and one movie and can be found with this article online at http://dx.doi.org/10.1016/j.cell.2013.06.052.

ACKNOWLEDGMENTS

We thank Rob Middleton for computer support; Rob Solomon, Steven Allen, Frank Kao, Suat Dervish, and Shi-Hong Yang for FACS; Qian Wang, Jessica Vanslambrouck, Kristina Jahn, Delfine Cheng, and Adrian Smith for microscopy; and Geneworks for next-generation sequencing. This study was supported by Cancer Council NSW (J.E.J.R., W.R. and J.H.), Rebecca L Cooper Medical Research Foundation (J.E.J.R. and J.H.), National Health and Medical Research Council (W.R.; 571156), Cancer Institute of NSW (W.R. and J.W.H.W), National Breast Cancer Foundation (J.H.), Tour de Cure (C.G.B. and J.E.J.R), Cure the Future (J.J.-L.W. and J.E.J.R.) and an anonymous foundation (J.E.J.R.).

Received: November 21, 2012
Revised: May 1, 2013
Accepted: June 28, 2013
Published: August 1, 2013

REFERENCES

Alló, M., Buggiano, V., Fededa, J.P., Petrillo, E., Schor, I., de la Mata, M., Agirre, E., Plass, M., Eyras, E., Elela, S.A., et al. (2009). Control of alternative splicing through siRNA-mediated transcriptional gene silencing. Nat. Struct. Mol. Biol. *16*, 717–724.

Altschul, S.F., Gish, W., Miller, W., Myers, E.W., and Lipman, D.J. (1990). Basic local alignment search tool. J. Mol. Biol. *215*, 403–410.

Amit, M., Donyo, M., Hollander, D., Goren, A., Kim, E., Gelfman, S., Lev-Maor, G., Burstein, D., Schwartz, S., Postolsky, B., et al. (2012). Differential GC content between exons and introns establishes distinct strategies of splice-site recognition. Cell Rep. *1*, 543–556.

Audic, S., and Claverie, J.M. (1997). The significance of digital gene expression profiles. Genome Res. *7*, 986–995.

Belgrader, P., Cheng, J., Zhou, X., Stephenson, L.S., and Maquat, L.E. (1994). Mammalian nonsense codons can be cis effectors of nuclear mRNA half-life. Mol. Cell. Biol. *14*, 8219–8228.

Bell, T.J., Miyashiro, K.Y., Sul, J.-Y., McCullough, R., Buckley, P.T., Jochems, J., Meaney, D.F., Haydon, P., Cantor, C., Parsons, T.D., and Eberwine, J. (2008). Cytoplasmic BK(Ca) channel intron-containing mRNAs contribute to the intrinsic excitability of hippocampal neurons. Proc. Natl. Acad. Sci. USA *105*, 1901–1906.

Bell, T.J., Miyashiro, K.Y., Sul, J.-Y., Buckley, P.T., Lee, M.T., McCullough, R., Jochems, J., Kim, J., Cantor, C.R., Parsons, T.D., and Eberwine, J.H. (2010). Intron retention facilitates splice variant diversity in calcium-activated big potassium channel populations. Proc. Natl. Acad. Sci. USA *107*, 21152–21157.

Beltran, M., Puig, I., Peña, C., García, J.M., Álvarez, A.B., Peña, R., Bonilla, F., and de Herreros, A.G. (2008). A natural antisense transcript regulates Zeb2/Sip1 gene expression during Snail1-induced epithelial-mesenchymal transition. Genes Dev. *22*, 756–769.

Berg, M.G., Singh, L.N., Younis, I., Liu, Q., Pinto, A.M., Kaida, D., Zhang, Z., Cho, S., Sherrill-Mix, S., Wan, L., and Dreyfuss, G. (2012). U1 snRNP determines mRNA length and regulates isoform expression. Cell *150*, 53–64.

Bicknell, A.A., Cenik, C., Chua, H.N., Roth, F.P., and Moore, M.J. (2012). Introns in UTRs: why we should stop ignoring them. Bioessays *34*, 1025–1034.

Black, D.L. (2000). Protein diversity from alternative splicing: a challenge for bioinformatics and post-genome biology. Cell *103*, 367–370.

Buckley, P.T., Lee, M.T., Sul, J.-Y., Miyashiro, K.Y., Bell, T.J., Fisher, S.A., Kim, J., and Eberwine, J. (2011). Cytoplasmic intron sequence-retaining transcripts can be dendritically targeted via ID element retrotransposons. Neuron *69*, 877–884.

Dechat, T., Pfleghaar, K., Sengupta, K., Shimi, T., Shumaker, D.K., Solimando, L., and Goldman, R.D. (2008). Nuclear lamins: major factors in the structural organization and function of the nucleus and chromatin. Genes Dev. *22*, 832–853.

Guibal, F.C., Alberich-Jorda, M., Hirai, H., Ebralidze, A., Levantini, E., Di Ruscio, A., Zhang, P., Santana-Lemos, B.A., Neuberg, D., Wagers, A.J., et al. (2009). Identification of a myeloid committed progenitor as the cancer-initiating cell in acute promyelocytic leukemia. Blood *114*, 5415–5425.

Hentze, M.W., and Kulozik, A.E. (1999). A perfect message: RNA surveillance and nonsense-mediated decay. Cell *96*, 307–310.

Hillman, R.T., Green, R.E., and Brenner, S.E. (2004). An unappreciated role for RNA surveillance. Genome Biol. *5*, R8.

Hobert, O. (2008). Gene regulation by transcription factors and microRNAs. Science *319*, 1785–1786.

Hofacker, I.L. (2009). RNA secondary structure analysis using the Vienna RNA package. Curr. Protoc. Bioinformatics *26*, 12.2.1–12.2.16.

Hoffmann, K., Dreger, C.K., Olins, A.L., Olins, D.E., Shultz, L.D., Lucke, B., Karl, H., Kaps, R., Müller, D., Vayá, A., et al. (2002). Mutations in the gene encoding the lamin B receptor produce an altered nuclear morphology in granulocytes (Pelger-Huët anomaly). Nat. Genet. *31*, 410–414.

Holst, J., Szymczak-Workman, A.L., Vignali, K.M., Burton, A.R., Workman, C.J., and Vignali, D.A.A. (2006a). Generation of T-cell receptor retrogenic mice. Nat. Protoc. *1*, 406–417.

Holst, J., Vignali, K.M., Burton, A.R., and Vignali, D.A.A. (2006b). Rapid analysis of T-cell selection in vivo using T cell-receptor retrogenic mice. Nat. Methods *3*, 191–197.

Houben, F., Ramaekers, F.C.S., Snoeckx, L.H.E.H., and Broers, J.L.V. (2007). Role of nuclear lamina-cytoskeleton interactions in the maintenance of cellular strength. Biochim. Biophys. Acta *1773*, 675–686.

Huang, W., Sherman, B.T., and Lempicki, R.A. (2009). Systematic and integrative analysis of large gene lists using DAVID bioinformatics resources. Nat. Protoc. *4*, 44–57.

Ivanov, I., Lo, K.C., Hawthorn, L., Cowell, J.K., and Ionov, Y. (2007). Identifying candidate colon cancer tumor suppressor genes using inhibition of nonsense-mediated mRNA decay in colon cancer cells. Oncogene *26*, 2873–2884.

Ji, J.Y., Lee, R.T., Vergnes, L., Fong, L.G., Stewart, C.L., Reue, K., Young, S.G., Zhang, Q., Shanahan, C.M., and Lammerding, J. (2007). Cell nuclei spin in the absence of lamin B1. J. Biol. Chem. *282*, 20015–20026.

Kaida, D., Berg, M.G., Younis, I., Kasim, M., Singh, L.N., Wan, L., and Dreyfuss, G. (2010). U1 snRNP protects pre-mRNAs from premature cleavage and polyadenylation. Nature *468*, 664–668.

Kalyna, M., Simpson, C.G., Syed, N.H., Lewandowska, D., Marquez, Y., Kusenda, B., Marshall, J., Fuller, J., Cardle, L., McNicol, J., et al. (2012). Alternative splicing and nonsense-mediated decay modulate expression of important regulatory genes in Arabidopsis. Nucleic Acids Res. *40*, 2454–2469.

Kanehisa, M., Goto, S., Sato, Y., Furumichi, M., and Tanabe, M. (2012). KEGG for integration and interpretation of large-scale molecular data sets. Nucleic Acids Res. *40*(Database issue), D109–D114.

Kishore, S., and Stamm, S. (2006). The snoRNA HBII-52 regulates alternative splicing of the serotonin receptor 2C. Science *311*, 230–232.

Lammerding, J., Fong, L.G., Ji, J.Y., Reue, K., Stewart, C.L., Young, S.G., and Lee, R.T. (2006). Lamins A and C but not lamin B1 regulate nuclear mechanics. J. Biol. Chem. *281*, 25768–25780.

Lee, G., Foerster, J., Lukens, J., Paraskevas, F., Greer, J., and Rogers, G. (1999). Wintrobe's Clinical Hematology, 10 edn (Baltimore: William and Wilkins).

Lejeune, F., and Maquat, L.E. (2005). Mechanistic links between nonsense-mediated mRNA decay and pre-mRNA splicing in mammalian cells. Curr. Opin. Cell Biol. *17*, 309–315.

Lev-Maor, G., Ram, O., Kim, E., Sela, N., Goren, A., Levanon, E.Y., and Ast, G. (2008). Intronic Alus influence alternative splicing. PLoS Genet. *4*, e1000204.

Lian, Z., Kluger, Y., Greenbaum, D.S., Tuck, D., Gerstein, M., Berliner, N., Weissman, S.M., and Newburger, P.E. (2002). Genomic and proteomic analysis of the myeloid differentiation program: global analysis of gene expression during induced differentiation in the MPRO cell line. Blood *100*, 3209–3220.

Luco, R.F., Pan, Q., Tominaga, K., Blencowe, B.J., Pereira-Smith, O.M., and Misteli, T. (2010). Regulation of alternative splicing by histone modifications. Science *327*, 996–1000.

Malhas, A., Lee, C.F., Sanders, R., Saunders, N.J., and Vaux, D.J. (2007). Defects in lamin B1 expression or processing affect interphase chromosome position and gene expression. J. Cell Biol. *176*, 593–603.

Malhas, A., Saunders, N.J., and Vaux, D.J. (2010). The nuclear envelope can control gene expression and cell cycle progression via miRNA regulation. Cell Cycle *9*, 531–539.

Martin, C., Chen, S., Maya-Mendoza, A., Lovric, J., Sims, P.F.G., and Jackson, D.A. (2009). Lamin B1 maintains the functional plasticity of nucleoli. J. Cell Sci. *122*, 1551–1562.

Neu-Yilik, G., Amthor, B., Gehring, N.H., Bahri, S., Paidassi, H., Hentze, M.W., and Kulozik, A.E. (2011). Mechanism of escape from nonsense-mediated mRNA decay of human β-globin transcripts with nonsense mutations in the first exon. RNA *17*, 843–854.

Ni, J.Z., Grate, L., Donohue, J.P., Preston, C., Nobida, N., O'Brien, G., Shiue, L., Clark, T.A., Blume, J.E., and Ares, M., Jr. (2007). Ultraconserved elements are associated with homeostatic control of splicing regulators by alternative splicing and nonsense-mediated decay. Genes Dev. *21*, 708–718.

Novershtern, N., Subramanian, A., Lawton, L.N., Mak, R.H., Haining, W.N., McConkey, M.E., Habib, N., Yosef, N., Chang, C.Y., Shay, T., et al. (2011). Densely interconnected transcriptional circuits control cell states in human hematopoiesis. Cell *144*, 296–309.

Olins, A.L., Herrmann, H., Lichter, P., Kratzmeier, M., Doenecke, D., and Olins, D.E. (2001). Nuclear envelope and chromatin compositional differences comparing undifferentiated and retinoic acid- and phorbol ester-treated HL-60 cells. Exp. Cell Res. *268*, 115–127.

Olins, A.L., Zwerger, M., Herrmann, H., Zentgraf, H., Simon, A.J., Monestier, M., and Olins, D.E. (2008). The human granulocyte nucleus: Unusual nuclear envelope and heterochromatin composition. Eur. J. Cell Biol. *87*, 279–290.

Padgett, R.A., Mount, S.M., Steitz, J.A., and Sharp, P.A. (1983). Splicing of messenger RNA precursors is inhibited by antisera to small nuclear ribonucleoprotein. Cell *35*, 101–107.

Pan, Q., Shai, O., Lee, L.J., Frey, B.J., and Blencowe, B.J. (2008). Deep surveying of alternative splicing complexity in the human transcriptome by high-throughput sequencing. Nat. Genet. *40*, 1413–1415.

Peric-Hupkes, D., Meuleman, W., Pagie, L., Bruggeman, S.W.M., Solovei, I., Brugman, W., Gräf, S., Flicek, P., Kerkhoven, R.M., van Lohuizen, M., et al. (2010). Molecular maps of the reorganization of genome-nuclear lamina interactions during differentiation. Mol. Cell *38*, 603–613.

Rosenbauer, F., and Tenen, D.G. (2007). Transcription factors in myeloid development: balancing differentiation with transformation. Nat. Rev. Immunol. *7*, 105–117.

Schwanhäusser, B., Busse, D., Li, N., Dittmar, G., Schuchhardt, J., Wolf, J., Chen, W., and Selbach, M. (2011). Global quantification of mammalian gene expression control. Nature *473*, 337–342.

Shao, W., Kim, H.-S., Cao, Y., Xu, Y.-Z., and Query, C.C. (2012). A U1-U2 snRNP interaction network during intron definition. Mol. Cell. Biol. *32*, 470–478.

Shi, J., Hu, Z., Pabon, K., and Scotto, K.W. (2008). Caffeine regulates alternative splicing in a subset of cancer-associated genes: a role for SC35. Mol. Cell. Biol. *28*, 883–895.

Shimi, T., Butin-Israeli, V., Adam, S.A., Hamanaka, R.B., Goldman, A.E., Lucas, C.A., Shumaker, D.K., Kosak, S.T., Chandel, N.S., and Goldman, R.D. (2011). The role of nuclear lamin B1 in cell proliferation and senescence. Genes Dev. *25*, 2579–2593.

Sultan, M., Schulz, M.H., Richard, H., Magen, A., Klingenhoff, A., Scherf, M., Seifert, M., Borodina, T., Soldatov, A., Parkhomchuk, D., et al. (2008). A global view of gene activity and alternative splicing by deep sequencing of the human transcriptome. Science *321*, 956–960.

Taft, R.J., Simons, C., Nahkuri, S., Oey, H., Korbie, D.J., Mercer, T.R., Holst, J., Ritchie, W., Wong, J.J.L., Rasko, J.E.J., et al. (2010). Nuclear-localized tiny RNAs are associated with transcription initiation and splice sites in metazoans. Nat. Struct. Mol. Biol. *17*, 1030–1034.

Tang, C.W., Maya-Mendoza, A., Martin, C., Zeng, K., Chen, S., Feret, D., Wilson, S.A., and Jackson, D.A. (2008). The integrity of a lamin-B1-dependent nucleoskeleton is a fundamental determinant of RNA synthesis in human cells. J. Cell Sci. *121*, 1014–1024.

Theilgaard-Mönch, K., Jacobsen, L.C., Borup, R., Rasmussen, T., Bjerregaard, M.D., Nielsen, F.C., Cowland, J.B., and Borregaard, N. (2005). The transcriptional program of terminal granulocytic differentiation. Blood *105*, 1785–1796.

Trapnell, C., Williams, B.A., Pertea, G., Mortazavi, A., Kwan, G., van Baren, M.J., Salzberg, S.L., Wold, B.J., and Pachter, L. (2010). Transcript assembly and quantification by RNA-Seq reveals unannotated transcripts and isoform switching during cell differentiation. Nat. Biotechnol. *28*, 511–515.

Vergnes, L., Péterfy, M., Bergo, M.O., Young, S.G., and Reue, K. (2004). Lamin B1 is required for mouse development and nuclear integrity. Proc. Natl. Acad. Sci. USA *101*, 10428–10433.

Ward, A.C., Loeb, D.M., Soede-Bobok, A.A., Touw, I.P., and Friedman, A.D. (2000). Regulation of granulopoiesis by transcription factors and cytokine signals. Leukemia *14*, 973–990.

Weischenfeldt, J., Damgaard, I., Bryder, D., Theilgaard-Mönch, K., Thoren, L.A., Nielsen, F.C., Jacobsen, S.E.W., Nerlov, C., and Porse, B.T. (2008). NMD is essential for hematopoietic stem and progenitor cells and for eliminating by-products of programmed DNA rearrangements. Genes Dev. *22*, 1381–1396.

Yamashita, A., Ohnishi, T., Kashima, I., Taya, Y., and Ohno, S. (2001). Human SMG-1, a novel phosphatidylinositol 3-kinase-related protein kinase, associates with components of the mRNA surveillance complex and is involved in the regulation of nonsense-mediated mRNA decay. Genes Dev. *15*, 2215–2228.

Yang, S.H., Chang, S.Y., Yin, L., Tu, Y., Hu, Y., Yoshinaga, Y., de Jong, P.J., Fong, L.G., and Young, S.G. (2011). An absence of both lamin B1 and lamin B2 in keratinocytes has no effect on cell proliferation or the development of skin and hair. Hum. Mol. Genet. *20*, 3537–3544.

Zhang, J., and Maquat, L.E. (1997). Evidence that translation reinitiation abrogates nonsense-mediated mRNA decay in mammalian cells. EMBO J. *16*, 826–833.